

longitudinal photons via the one-pion-exchange diagram. The data of this experiment taken in conjunction with the photoproduction 90° cross section are suggestive of a similar contribution at large momentum transfer. This again can be contrasted to the simple quark model which predicts that only transverse photons will contribute. The data can be understood simply in terms of a vector-dominance-like model in which the Q^2 dependence is given by the ρ propagator and the W dependence is the same as that observed in $\pi p \rightarrow \pi p$ elastic scattering.

In conclusion, we have observed the W dependence of Reaction (3) at 90° to be in agreement with the prediction of the parton-interchange model. However, it seems difficult to explain the observed Q^2 dependence within the framework of this model.

We wish to acknowledge the support of Professor Boyce McDaniel, the staff of the Wilson Syn-

chrotron Laboratory, and the staff of the Harvard High Energy Physics Laboratory.

*Research supported in part by the U. S. Energy Research and Development Administration (Harvard) and the National Science Foundation (Cornell).

†Present address: Clinton P. Anderson Laboratory, Los Alamos, New Mex. 87545.

¹R. Talman, in *Proceedings of the International Symposium on Electron and Photon Interactions at High Energy, Bonn, Germany, 1973*, edited by H. Rollnick and W. Pfeil (North-Holland, Amsterdam, 1974), p. 145.

²C. J. Bebek *et al.*, Phys. Rev. D **9**, 1229 (1974).

³F. A. Berends, Phys. Rev. D **1**, 2590 (1970).

⁴S. J. Brodsky and G. R. Farrar, Phys. Rev. Lett. **31**, 1153 (1973).

⁵A. Bartl and P. Urban, Acta Phys. Austriaca **24**, 139 (1966).

⁶R. L. Anderson *et al.*, Phys. Rev. Lett. **30**, 627 (1973).

⁷G. Buschhorn *et al.*, Phys. Rev. Lett. **18**, 571 (1967).

Measurement of Neutrino and Antineutrino Total Cross Sections at High Energy*

B. C. Barish, J. F. Bartlett, D. Buchholz, T. Humphrey, F. S. Merritt, F. J. Sciulli,
L. Stutte, D. Shields, and H. Suter†

California Institute of Technology, Pasadena, California 91125

and

E. Fisk and G. Krafczyk

Fermi National Accelerator Laboratory, Batavia, Illinois 60510

(Received 2 September 1975)

Charged-current ν and $\bar{\nu}$ data are reported from the first application at Fermilab of a narrow-band neutrino beam for the measurement of normalized cross sections. Cross sections of about 20% accuracy were measured with a 120-GeV secondary hadron beam for ν ($\bar{\nu}$) originating from π decay ($\langle E_\nu \rangle = 38$ GeV) and K decay ($\langle E_\nu \rangle = 105$ GeV). The ν and $\bar{\nu}$ fluxes were determined by directly measuring the hadron flux and the $\pi/K/p$ ratios for the hadron beam.

The usual local current-current weak-interaction theory predicts that the neutrino-lepton cross section at high energy rises linearly with laboratory energy. If, in addition, the deep-inelastic structure functions scale in the dimensionless scaling variable x , the neutrino-nucleon cross section must rise linearly with laboratory energy as well.¹ The behavior of the total neutrino (antineutrino) charged-current cross section σ_ν ($\sigma_{\bar{\nu}}$) on nucleons,

$$\nu_\mu (\bar{\nu}_\mu) + N \rightarrow \mu^- (\mu^+) + \text{hadrons},$$

therefore provides simultaneously a directly in-

terpretable check of both weak-interaction theory and scaling.

Neutrino and antineutrino cross sections² previously measured at low energies ($E_\nu \lesssim 8$ GeV) are consistent with a linear rise in energy. The best-fit slopes are $\alpha_\nu = 0.74 \pm 0.03$ and $\alpha_{\bar{\nu}} = 0.28 \pm 0.01$, where all α 's are in units of 10^{-38} cm²/GeV. We describe here a measurement of σ_ν and $\sigma_{\bar{\nu}}$ at higher energy in which the neutrino flux has been measured directly in the same experiment. (Preliminary results from this experiment have been presented earlier.³)

This is the first application of a narrow-band

neutrino beam for the measurement of normalized neutrino cross sections.⁴ The Fermilab narrow-band beam, utilized in this experiment, has been described elsewhere.⁵ The arrangement is shown in Fig. 1. Briefly, secondaries produced near 0 mrad by 300-GeV protons are charge and momentum analyzed and focused into a parallel beam of adjustable central momentum and approximate acceptance $\Delta\Omega \Delta p/p = 450 \mu\text{sr} \%$, $\Delta p/p = 36\%$ (full width at half-maximum). This beam is directed down a 345-m evacuated decay pipe in which the decays $\pi(K) \rightarrow \mu + \nu_\mu$ yield a neutrino energy spectrum in the forward direction that contains two bands of muon neutrinos (or antineutrinos)⁴⁻⁶ differing in mean energy by about a factor of 3. The pion neutrino band has a width of ± 10 GeV, and the kaon band has width of ± 18 GeV. (Typical measured spectra are given by Barish *et al.*⁷)

The total-cross-section data for ν_μ ($\bar{\nu}_\mu$) incident on iron nuclei were obtained with use of 300-GeV protons and 120-GeV secondaries. The neutrino data (from π^+ and K^+) and antineutrino data (from π^- and K^-) are based on 2.6×10^{16} and 4.0×10^{16} incident protons, respectively.

The scheme for directly measuring the neutrino total cross sections required measurements of the neutrino flux, detection efficiency, and event rate. The neutrino flux was determined⁶ by measuring the hadron secondary-beam intensity and the $\pi/K/p$ ratio in the beam. By use of the known geometry of the detection apparatus the flux was then determined directly within the systematic errors described below. The detection efficiency, again within the stated systematic errors, was evaluated from the measured differential distributions.

The total intensity of the secondary hadron beam was continuously measured at the end of the decay pipe with a 35-cm \times 50-cm ionization chamber (SIC), large enough to contain the full secondary beam (10 cm \times 22 cm). This monitor was calibrated against a secondary emission monitor (SEM) in the extracted proton beam by transport-

ing the primary proton beam through the beam elements (without target) and through the entire decay region. (The SEM, previously calibrated with various standards, was checked by foil irradiation during this run and found to correspond to its calibration to better than 5%.) The hadron beam was steered into the SIC with a 2.5-cm \times 5.0-cm scintillation monitor located on the axis of the SIC; this centering was continuously monitored under computer control.

The fraction of pions, kaons, and protons in this beam was determined with a Cherenkov counter⁶ located downstream of the decay region where a portion of the secondary beam was allowed to exit. These measurements were taken in the secondary beam under the same conditions of targeting, focusing, and steering as for normal neutrino data taking. The incident proton intensity, however, was lowered from the normal $(1-3) \times 10^{12}$ to $(2-3) \times 10^9$ protons/pulse to allow counting of individual particles in the secondary beam. Measurements of the particle fractions were made with positive and negative secondaries at a variety of beam energies. The results of this survey have been discussed elsewhere.⁶

The flux of neutrinos into the apparatus was then calculated directly, by use of the known location of the detection apparatus relative to the decay pipe, the flux of parent particles as measured above, the known particle momenta and lifetimes, and two-body decay kinematics. Table I gives the neutrino flux into the fiducial volume with the estimated systematic error. This error comes primarily from measurements of the particle ratios, and overall particle calibration of the SIC.

The neutrino target consisted of 160 tons of Fe instrumented to detect the interaction products. The steel was segmented into 1.5-m \times 1.5-m \times 10-cm slabs and interspersed with scintillation counters (used as a sampling calorimeter to measure hadron energy, E_h) and spark chambers (to follow the muon trajectory). A 1.5-m-diam iron-

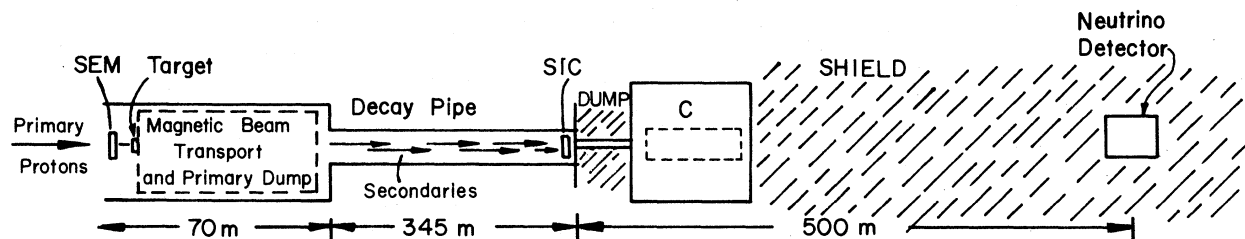


FIG. 1. Schematic of the experimental setup (not drawn to scale). The incident proton flux is monitored by the secondary emission monitor (SEM) immediately upstream of the target, and the secondary flux is monitored by the secondary ion chamber (SIC) at the end of the decay pipe.

core magnet, a large spark-chamber array, and trigger counters followed the target to determine the muon energy, E_μ . The apparatus was triggered by either (1) a muon traversing the magnet, or (2) significant energy deposition in the sam-

pling calorimeter (>99% efficient for $E_h > 6$ GeV). Roughly 90% of all neutrinos interacting inside the 127-cm \times 127-cm fiducial volume satisfy at least one of these triggers.

The neutrino cross section was obtained from the restricted sample of observed events (about 50%) having a final-state muon traversing the iron-core magnet. Both muon and hadron energies were measured for this sample, yielding the total energy ($E_\nu = E_h + E_\mu$) for each event and thus determining whether the incident neutrino originated from a pion decay or from a kaon decay. The number of events, T , in each category, after small corrections for the finite (~25%) energy resolution, is given in Table I.

These events were then corrected by the detection efficiency, ϵ , for having the muon traverse the magnet. This efficiency was determined from the sample of all triggering events by empirically fitting the angular distribution by the following form.

$$dN^\nu/dx dy = CF_2^{ed}(x)[1 + a_\nu(1-y)^2], \quad (1)$$

$$dN^{\bar{\nu}}/dx dy = CF_2^{ed}(x)[a_{\bar{\nu}} + (1-y)^2], \quad (2)$$

where $x = Q^2/2ME_h$, $y = E_h/E_\nu$, and $Q^2 = 4E_\nu E_\mu \times \sin^2\theta/2$. M is the nucleon mass, θ is the muon scattering angle, and $F_2^{ed}(x)$ is the structure function measured in electron-deuteron scattering.⁸ It is expected from charge symmetry that $a_\nu = a_{\bar{\nu}}$.⁹ A comparison of the angular distribution of the outgoing muons for all events (including those where the muon missed the magnet) with the distribution expected from Eqs. (1) and (2) yielded $a_\nu = 0.1^{+0.4}_{-0.2}$ and $a_{\bar{\nu}} = 0.25^{+0.5}_{-0.2}$. The detection efficiency for traversing the magnet shown in Table I along with an associated systematic error was evaluated with use of the average value¹⁰ $a_\nu = a_{\bar{\nu}} = 0.17^{+0.30}_{-0.15}$.

The total neutrino cross section per nucleon was obtained from the relation $\sigma_{tot} = T/FB\epsilon$ where T is the total number of observed interacting neutrinos with measured final muon energy, ϵ is the efficiency for the muon to traverse the magnet, F is the total number of incident neutrinos, and $B = 3.087 \times 10^{27}$ nucleons/cm². The resulting total cross sections with the associated statistical and total errors are shown in Table I.

In Fig. 2 the cross sections measured in this experiment are compared to the low-energy data² from the CERN bubble chamber Gargamelle. The data are consistent with a cross section rising linearly with energy ($\sigma_{tot} = \alpha E_\nu$). The best-fit

TABLE I. The cross sections per nucleon (σ_{tot}) for ν ($\bar{\nu}$) on an Fe target. Also shown are the values of the detection efficiency (ϵ), number of events (T), neutrino flux (F), and associated statistical and systematic uncertainties.

Parent Particle	Mean E_μ (GeV)	ϵ	$(\frac{\Delta\epsilon}{\epsilon})_{sys}$	T (events)	$(\frac{\Delta T}{T})_{sys}$	$(\frac{\Delta T}{T})_{stat}$	$F \times 10^{11}$ (neutrinos)	$(\frac{\Delta F}{F})_{sys}$	σ_{tot}^{tot} (10^{-38} cm ²)	ΔC stat	ΔC total
π^+	38	.326	.066	233.6	.073	.061	7.77	.13	29.9	1.8	5.2
K^+	107	.454	.052	102.8	.078	.092	.74	.16	98.6	9.1	20.4
π^-	38	.529	.164	97.6	.049	.097	5.02	.11	11.9	1.2	2.7
K^-	102	.647	.125	10.9	.181	.29	.24	.18	22.9	6.6	9.3

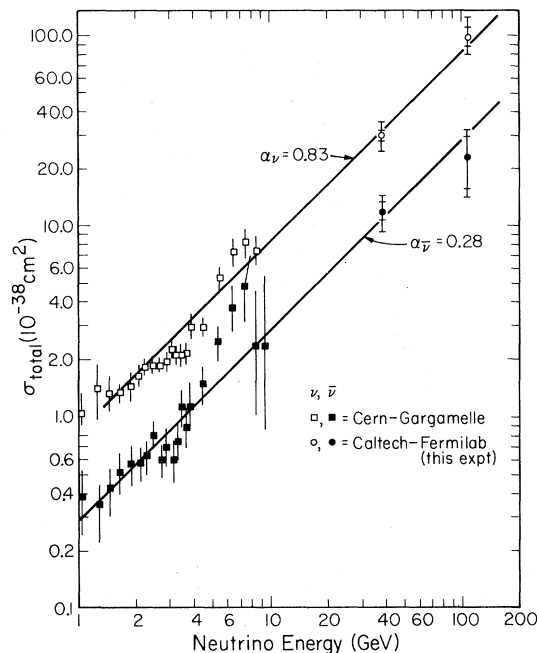


FIG. 2. Comparison of this experiment to the low-energy Gargamelle data. The inner error bars on the California Institute of Technology (Caltech)-Fermilab points correspond to statistical error only. The outer bars include the estimated systematic error added in quadrature. The slopes quoted on the figure are best fits to the Caltech-Fermilab data above.

slopes from this experiment alone are

$$\alpha_{\nu} = (0.83 \pm 0.11) \times 10^{-38} \text{ cm}^2/\text{GeV}, \quad (3)$$

$$\alpha_{\bar{\nu}} = (0.28 \pm 0.055) \times 10^{-38} \text{ cm}^2/\text{GeV}. \quad (4)$$

The Gargamelle data are in agreement with this fit. Other high-energy neutrino data,¹¹ obtained with the broad-band horn-focused beam at Fermilab and normalized to "quasi-elastic" events, also agree with the above slope to within a standard deviation.

The results presented here are significant in three major respects: (1) The observed linear rise in cross section supports a current-current interaction and scaling of the nucleon structure functions. (2) The ratio of neutrino to antineutrino cross sections is consistent with the value of approximately 3 expected from a predominant $V-A$ coupling to the quark component of the nucleon.¹² (3) The sum of the slopes $\alpha_{\nu} + \alpha_{\bar{\nu}}$ is related to the electromagnetic structure function measured in deep-inelastic $e-d$ scattering [see Eqs. (1) and (2)] and in parton models measures the mean square charge of the constituent partons.¹² The slopes given above are consistent with the fractional charges expected in the sim-

plest quark model.

The first application of the narrow-band beam technique for the measurement of normalized cross sections has been extremely encouraging. The simple flux-measuring techniques applied in this initial run have provided overall accuracies of between 10 and 20% in the normalization. By improving critical areas and providing redundancy in others, we expect that the fluxes will be measured to about 5% in the near future. In the longer term, improvements in the neutrino detection apparatus and the narrow-band beam transport should ultimately give overall cross sections to match this accuracy.

This experiment, involving readout and control equipment staged over very long distances, necessarily entails rather strong interaction between experimental and accelerator personnel. We express our gratitude to the Accelerator and Neutrino Laboratory staff for help and favors, past, present, and future.

*Work supported in part by the U. S. Energy Research and Development Administration. Prepared under Contract No. AT(11-1)-68 for the San Francisco Operations Office.

†Swiss National Fund for Scientific Research Fellow.

¹J. D. Bjorken, *Phys. Rev.* **179**, 1547 (1969).

²T. Eichen *et al.*, *Phys. Lett.* **46B**, 274, 281 (1973).

³F. Sciulli, in *Proceedings of the Seventeenth International Conference on High Energy Physics, London, England, 1974*, edited by J. R. Smith (Rutherford High Energy Laboratory, Didcot, Berkshire, England, 1975), p. IV-105.

⁴B. C. Barish *et al.*, FNAL Proposal No. E-21, 1970 (unpublished).

⁵P. Limon *et al.*, *Nucl. Instrum. Methods* **116**, 317 (1974). Also see Ref. 4.

⁶T. Humphrey, Ph.D. thesis, California Institute of Technology, 1975 (unpublished).

⁷B. C. Barish *et al.*, *Phys. Rev. Lett.* **32**, 1387 (1974); F. Sciulli, Ref. 3, and in "Neutrino '75," *Proceedings of the International Conference on Particle Physics, Balatonfured, Hungary, June 1975* (to be published).

⁸A. Bodek, Ph.D. thesis, Massachusetts Institute of Technology, Laboratory for Nuclear Science Report No. LNS-COO-3069-116, 1972 (unpublished).

⁹In general α_{ν} and $\alpha_{\bar{\nu}}$ are functions of x . The x dependence is being studied by use of a larger sample of deep-inelastic-scattering data and those results will be reported elsewhere; preliminary results agree with the values used here.

¹⁰Previous neutrino data taken with the narrow-band beam are in good agreement with this value and yield $\alpha_{\nu} = 0.05 \pm_{0.17}^{0.25}$.

¹¹A. Benvenuti *et al.*, *Phys. Rev. Lett.* **32**, 125 (1974);

R. Imlay, in *Proceedings of the Seventeenth International Conference on High Energy Physics, London, England, 1974*, edited by J. R. Smith (Rutherford High Energy Laboratory, Didcot, Berkshire, England, 1975), p. V-50.

¹²R. P. Feynman, in *Neutrinos—1974*, edited by C. Bal-

tay, AIP Conference Proceedings No. 22 (American Institute of Physics, New York, 1974); D. C. Cundy, in *Proceedings of the Seventeenth International Conference on High Energy Physics, London, England, 1974*, edited by J. R. Smith (Rutherford High Energy Laboratory, Didcot, Berkshire, England, 1975), p. IV-131.

Azimuthal Asymmetry in Inclusive Hadron Production by e^+e^- Annihilation*

R. F. Schwitters, A. M. Boyarski, M. Breidenbach, F. Bulos, G. J. Feldman, G. Hanson, D. L. Hartill, B. Jean-Marie, R. R. Larsen, D. Lüke, † V. Lüth, H. L. Lynch, C. C. Morehouse, J. M. Paterson, M. L. Perl, T. P. Pun, P. Rapidis, B. Richter, W. Tanenbaum, and F. Vannucci‡
Stanford Linear Accelerator Center, Stanford University, Stanford, California 94305

and

F. M. Pierre, § G. S. Abrams, W. Chinowsky, C. E. Friedberg, G. Goldhaber, J. A. Kadyk, A. M. Litke, B. A. Lulu, B. Sadoulet, G. H. Trilling, J. S. Whitaker, F. C. Winkelmann, and J. E. Wiss
Lawrence Berkeley Laboratory and Department of Physics, University of California, Berkeley, California 94720
 (Received 18 August 1975)

We have observed an azimuthal asymmetry in inclusive hadron production by e^+e^- annihilation at the center-of-mass energy $\sqrt{s} = 7.4$ GeV. The asymmetry is caused by the polarization of the circulating beams in the storage ring and allows separate determination of the transverse and longitudinal structure functions. We find that transverse production dominates for $x > 0.2$ where x is the scaling variable $2p/\sqrt{s}$.

The transverse beam polarization which is expected to arise in high-energy electron-positron storage rings¹ provides a convenient analyzer for studying the dynamics of electron-positron interactions. At SPEAR, significant beam polarization has been observed² at the c.m. energy $\sqrt{s} = 7.4$ GeV through the reaction $e^+e^- \rightarrow \mu^+\mu^-$. We report here measurements of inclusive hadron production (obtained simultaneously with these muon-pair data) which also show strong azimuthal-angle dependence, correlated with the initial-state polarization. The hadron azimuthal asymmetry is observed to have the same sign as μ -pair production, viz., hadrons are preferentially produced perpendicular to the polarization direction. This effect is momentum dependent; hadrons of low momenta show little polarization dependence, while the particles of highest momenta have azimuthal asymmetries comparable to muon pairs, which is the largest possible.

The beams are polarized with the electron (positron) spins predominantly aligned antiparallel (parallel) to the guide magnetic field of the storage ring. The dominant state formed by the annihilation of such polarized beams is that of a single, linearly polarized virtual photon. The

general angular distribution for any final-state particle produced through annihilation has the following simple form³:

$$d\sigma/d\Omega = \sigma_T + \sigma_L + (\sigma_T - \sigma_L) \cos^2\theta + P^2(\sigma_T - \sigma_L) \sin^2\theta \cos 2\varphi. \quad (1)$$

θ is the polar angle of the produced particle measured with respect to the incident positron direction, φ is the azimuthal angle measured from the horizontal plane (the polarization direction is vertical), P is the magnitude of the polarization of each beam, and σ_T and σ_L contain the transverse and longitudinal structure functions which describe the energy and momentum dependence of the production process. Although σ_L and σ_T can, in principle, be determined from the $\cos^2\theta$ terms even in the absence of polarization, the finite polar-angle acceptance of the apparatus (50–130°) severely limits the precision achievable in this manner. The polarization-dependent term in Eq. (1) leads to an azimuthal dependence which can be used to separate the structure functions into transverse and longitudinal components with much greater accuracy even if the polar-angle acceptance of the experiment is limited to angles